Operation Characteristic Analysis of an Asymmetrical Half-Bridge Converter with Half-Wave Rectifier

Yerin Lee, Jungho Jeon, and Paul Jang
Department of Energy and Electrical Engineering, Tech University of Korea, South Korea

***Abstract*—Generally, when designing a symmetrical half-bridge converter, the rectifier on the secondary side is composed of a full-bridge rectifier or a center-tap rectifier to take advantage of the full-wave rectifier (FWR). However, when driving with asymmetrical PWM, the benefit of full-wave rectification due to symmetric operation is lost, so a half-wave rectifier (HWR) can be introduced to cope with low-voltage and high-current applications. Furthermore, if an HWR is used with an asymmetrical half-bridge converter (AHBC), the soft switching characteristics of the AHBC can be improved while maintaining appropriate conduction loss. It is because the transformer current has a negative average with the reduced duty cycle loss due to the operation characteristics of HWR. Accordingly, this study examines the superiority of an AHBC with HWR in an efficiency aspect compared to the case of using FWR through the operation characteristic analysis. The validity of the analysis is verified through experiments with a 360-W prototype.**

***Index Terms*—asymmetrical half-bridge converter (AHBC), half-wave rectifier (HWR), soft switching.**

I. INTRODUCTION

Half-bridge converter is widely used in medium power level applications due to its simplicity and low voltage stresses on the transistors [1]-[8]. There are two types of pulse width modulation (PWM) implementation on half-bridge converter: 1) symmetrical control and 2) asymmetrical control. When using a symmetrical PWM in a half-bridge converter, the rectifier on the secondary side generally comprises a full-bridge rectifier or a center-tap rectifier to take advantage of the full-wave rectifier (FWR) [2]. In addition, by this practice, most studies have used FWRs even when driving half-bridge converters with asymmetric PWM [3]-[8]. However, when driving with asymmetrical PWM, the advantage of full-wave rectification due to symmetric operation is lost, so a half-wave rectifier (HWR) can also be introduced to cope with low-voltage and high-current applications.

An asymmetrical half-bridge converter (AHBC) is widely utilized when high efficiency or high power density needs to be achieved since soft switching of the transistors can be attained through the asymmetrical PWM [6]-[8]. However, using an HWR with AHBC can improve the soft switching characteristics of AHBC, which can also benefit the overall system efficiency. Still, such analysis has yet to be made in the literature to the best of the author's knowledge. Therefore, in this paper, the operation characteristics of an AHBC with HWR are analyzed from the viewpoint of efficiency improvement and verified through experiments, ultimately aiming to achieve high efficiency of AHBC without introducing any additional circuits.

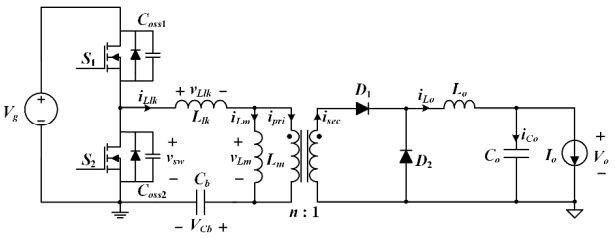

Fig. 1. Circuit configuration of an AHBC with HWR.

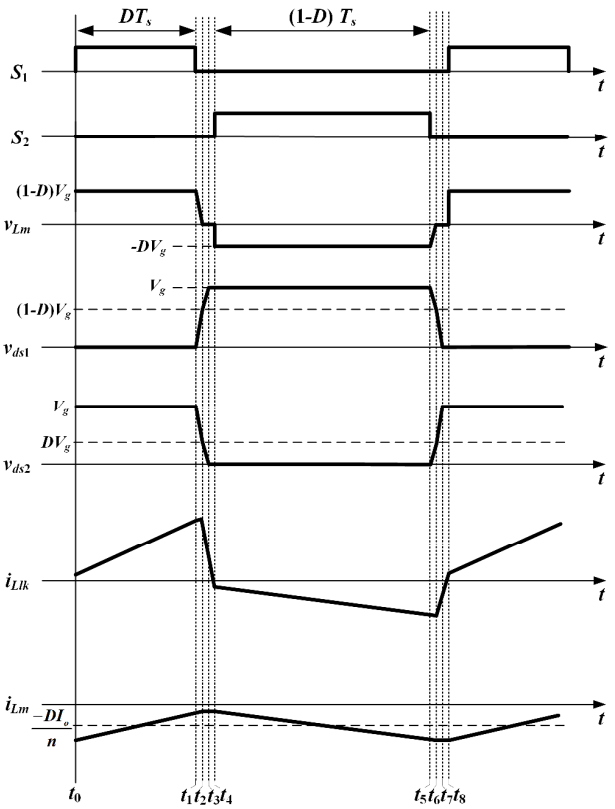

Fig. 2. Steady-state waveforms of an AHBC with an HWR.

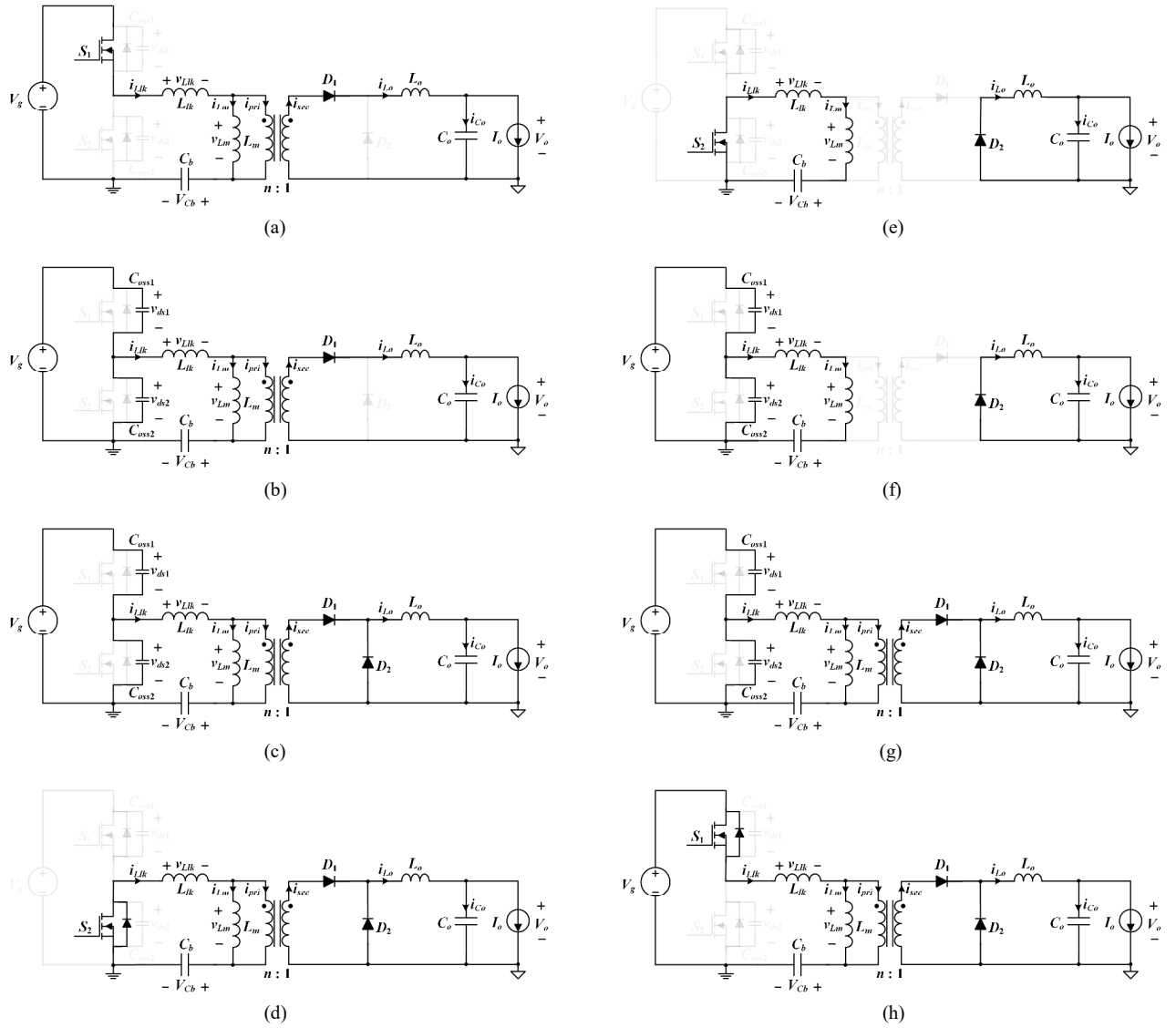

Fig. 3. Operation modes of an AHBC with HWR. (a) Mode 1, (b) Mode 2, (c) Mode 3, (d) Mode 4, (e) Mode 5, (f) Mode 6, (g) Mode 7, (h) Mode 8.

II. Operation Principle

The circuit configuration of an AHBC with HWR is shown in Fig. 1. The primary side circuit consists of bridge switches (S_1 and S_2), a blocking capacitor (C_b), and a transformer with a turn ratio of n. The transformer is modeled using the magnetizing inductance (L_m) and leakage inductance reflected on the primary side (L_{lk}). S_1 operates with the gate signal of the duty ratio (D), and S_2 operates in a complementary manner to the duty ratio of S_1 with dead times preceding and following each switch action. All switches include each body diode and output capacitor (C_{oss1} and C_{oss2}). The secondary side consists of two diodes (D_1 and D_2), an output inductor (L_o), and an output capacitor (C_o).

Fig. 2 shows the essential steady-state voltage and current waveforms of an AHBC with HWR operating in continuous-conduction mode (CCM). Under steady-state operation, each switching cycle is divided into eight intervals. When describing the circuit operation, the following will be assumed:

1) Switches are ideal, except for their body diodes and output capacitors;
2) L_{lk} is much less than L_m;
3) C_b is large enough to ignore its voltage ripple;
4) L_o is large enough to operate in CCM.

Mode 1[t_0-t_1]: In this mode, S_1 and D_1 are turned on, and S_2 and D_2 are turned off. Therefore, the energy is transferred from the primary to the secondary side. The voltage of V_g - V_{Cb} is applied to the primary side of the transformer.

Mode 2[t_1-t_2]: This mode starts when S_1 is turned off at t_1. The primary side forms a resonance network consisting of L_{lk}, L_m, C_{oss1}, and C_{oss2}. Hence, the voltage across C_{oss2} starts to discharge by the resonance. Here, the main source of this discharging comes from the load current. This mode lasts until the voltage across C_{oss2} becomes V_{Cb}.

Mode 3[t_2-t_3]: At t_2, the voltage across the primary and secondary of the transformer becomes 0. Therefore, L_m is excluded from the resonant network of mode 2, and the primary side operation is determined by the resonance network composed of L_{lk}, C_{oss1}, and C_{oss2}. In this mode, the

voltage of C_{oss2} is discharged by the energy stored in L_{lk}. When the energy to be discharged is sufficient and the voltage of C_{oss2} reaches 0, the condition for the body diode of S_2 to conduct is met. Then, this mode ends.

Mode 4[t_3-t_4]: Since the body diode of S_2 is conducting from t_3, S_2 can be turned on under zero-voltage switching (ZVS) condition. This mode lasts until the commutation between D_1 and D_2 is over.

Mode 5[t_4-t_5]: In mode 5, S_2 and D_2 are turned on, and S_1 and D_1 are turned off. In this mode, both the primary and secondary sides of the transformer operate as if the main switch is turned off in the buck converter, and S_2 and D_2 function as the freewheel conduction path.

Mode 6[t_5-t_6]: This mode starts when S_2 is turned off at t_5. The primary side forms a resonance network consisting of L_{lk}, L_m, C_{oss1}, and C_{oss2}. Hence, the voltage across C_{oss1} starts to discharge by the resonance. Here, the main source of this discharging comes from the magnetizing current. This mode lasts until the voltage across C_{oss1} becomes V_g - V_{Cb}.

Mode 7[t_6-t_7]: At t_7, the voltage across the primary and secondary of the transformer becomes 0. Therefore, L_m is excluded from the resonant network of mode 6, and the primary side operation is determined by the resonance network composed of L_{lk}, C_{oss1}, and C_{oss2}. In this mode, the voltage of C_{oss1} is discharged by the energy stored in L_{lk}. When the energy to be discharged is sufficient and the voltage of C_{oss1} reaches 0, the condition for the body diode of S_1 to conduct is met. Then, this mode ends.

Mode 8[t_7-t_8]: Since the body diode of S_1 is conducting from t_7, S_1 can be turned on under zero-voltage switching (ZVS) condition. This mode lasts until the commutation between D_1 and D_2 is over.

III. Analysis

A. Steady-State Analysis

If the dead times are ignored, the operation mode of an AHBC with HWR can be divided into two modes: mode 1 when S_1 is turned on; mode 5 when S_2 is turned on. Then, the following equations can be obtained by applying the voltage-second balance on the magnetizing inductor:

$$(V_g - V_{Cb})D - V_{Cb}(1-D) = 0\,, \tag{1}$$

Since the operation of the primary side is identical to that of a no-load synchronous buck converter, V_{Cb} can be calculated as if it were the output voltage of the buck converter:

$$V_{Cb} = DV_g\,. \tag{2}$$

If the voltage-second balance is applied to the output inductor again, the result is:

$$\left(\frac{V_g - V_{Cb}}{n} - V_o\right)D + (-V_o)(1-D) = 0\,. \tag{3}$$

Substituting (2) into (3), the voltage gain of an AHBC with HWR, M_{HWR}, is:

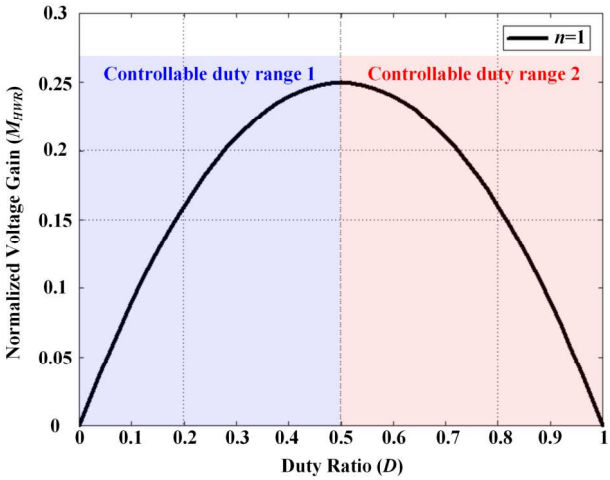

Fig. 4. Normalized voltage gain of an AHBC with HWR (n=1).

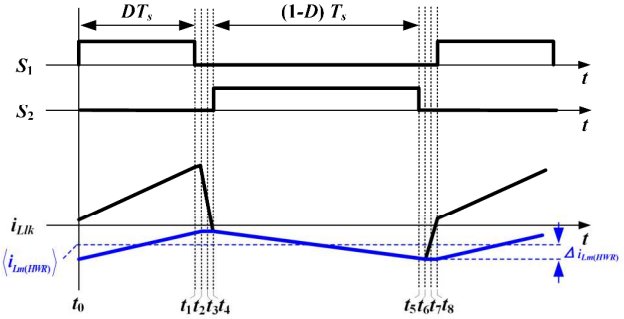

Fig. 5. Typical waveforms of an AHBC with HWR.

$$M_{HWR} = \frac{V_o}{V_g} = \frac{D(1-D)}{n}\,. \tag{4}$$

Fig. 4 shows the voltage gain of an AHBC with HWR according to (4). As can be seen, the duty range of 0 to 0.5 or 0.5 to 1 can be used theoretically, but using a small duty ratio range is advantageous in terms of transformer design to reduce loss and avoid saturation.

B. ZVS Analysis

Fig. 5 shows the typical current waveforms of an AHBC with HWR. Regarding Fig. 5, S_1 and S_2 each have different ZVS conditions.

First, for S_1, L_{lk}, C_{oss1}, and C_{oss2} resonate from the energy stored in L_{lk} at t_6, whereby C_{oss1} is discharged to achieve ZVS. From this, the ZVS condition of S_1 can be expressed as follow:

$$\frac{1}{2}L_{lk}\left[i_{Llk}(t_6)\right]^2 \geq \frac{1}{2}(C_{oss1} + C_{oss2})\left[(1-D)V_g\right]^2, \tag{5}$$

where $i_{Llk}(t_6)$ is the leakage inductor current at t_6, given as:

$$i_{Llk}(t_6) = \left\langle i_{Lm(HWR)} \right\rangle - \Delta i_{Lm(HWR)}\,. \tag{6}$$

If the charge balance in the blocking capacitor C_b is applied, the average magnetizing inductor current

TABLE I
SYSTEM SPECIFICATION

Input voltage (V_g)	400 V
Output voltage (V_o)	24 V
Rated output current (I_o)	15 A
Switching frequency (f_{sw})	100 kHz

TABLE II
DESIGN RESULTS OF AHBCS

Transformer turn ratio of an AHBC with HWR (n:1)	3:1
Transformer turn ratio of an AHBC with FWR (n:1:1)	6:1:1
Switch output capacitor (C_{oss})	100 pF
Blocking capacitor (C_b)	100 μF
Output capacitor (C_o)	200 μF
Output inductor (L_o)	47 μH

($<i_{Lm(HWR)}>$) and ripple ($\Delta i_{Lm(HWR)}$) can be obtained as follows:

$$\left(i_{Lm(HWR)}+\frac{i_{Lo}}{n}\right)D+i_{Lm(HWR)}(1-D)=0\,, \tag{7}$$

$$\left\langle i_{Lm(HWR)}\right\rangle=-\frac{I_o}{n}D\,, \tag{8}$$

$$\Delta i_{Lm(HWR)}=\frac{V_g D(1-D)T_s}{2L_m}\,. \tag{9}$$

Next, for S_2, L_{lk}, C_{oss1}, and C_{oss2} resonate from the energy stored in L_{lk} at t_2, whereby C_{oss2} is discharged to achieve ZVS. From this, the ZVS condition of S_2 can be expressed as follow:

$$\frac{1}{2}L_{lk}\left[i_{Llk}(t_2)\right]^2\geq\frac{1}{2}\left(C_{oss1}+C_{oss2}\right)\left(DV_g\right)^2\,, \tag{10}$$

where $i_{Llk}(t_2)$ is the leakage inductor current at t_2, given as:

$$i_{Llk}(t_2)=\left\langle i_{Lm(HWR)}\right\rangle+\frac{I_o}{n}+\Delta i_{Lm(HWR)}\,. \tag{11}$$

ZVS design can now be reflected in the worst case between (5) and (10). From the viewpoint of optimizing transformer design, if the duty range is 0 to 0.5, the absolute value of $i_{Llk}(t_6)$ is smaller between $i_{Llk}(t_2)$ and $i_{Llk}(t_6)$. Therefore, the ZVS condition of an AHBC with HWR can be summarized as

$$L_{lk}>\frac{2C_{oss}}{\left(\frac{DT_s}{2L_m}+\frac{I_o D}{n(1-D)V_g}\right)^2}\,, \tag{12}$$

if C_{oss1} and C_{oss2} are assumed to be C_{oss}.

C. Comparison with an AHBC with FWR

A comparative analysis with applying FWR is performed to compare how the characteristics of the AHBC change depending on the secondary rectifier. A center-tap rectifier

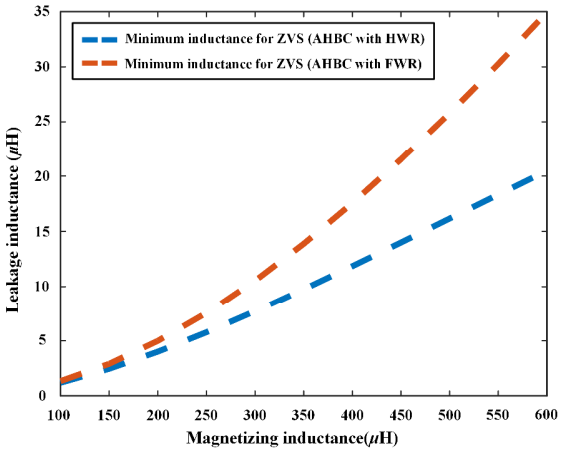

(a)

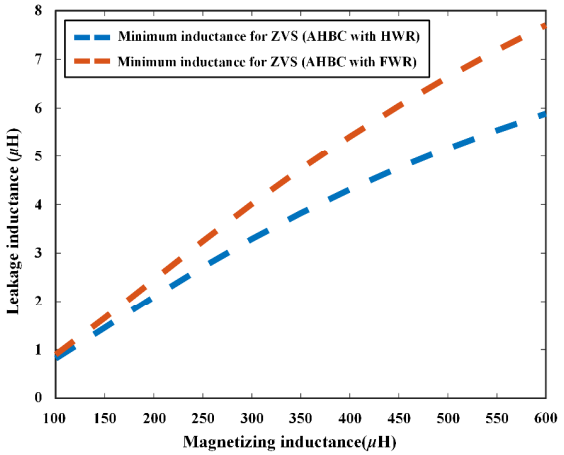

(b)

Fig. 6. Minimum L_{lk} for ZVS. (a) 30% load condition, (b) 100% load condition.

that features more similar to HWR was selected among the FWRs of a full-bridge rectifier or a center-tap rectifier in this study. Everything is the same as an AHBC with HWR except for using a center-tap transformer with a turn ratio of n:1:1 in the circuit configuration.

According to [4], the voltage gain of an AHBC with FWR, M_{FWR}, is:

$$M_{FWR}=\frac{V_o}{V_g}=\frac{2D(1-D)}{n}\,. \tag{13}$$

It can be seen from (4) and (13) that if an AHBC is designed with the same specification, an AHBC with FWR should have two times the transformer turn ratio than an AHBC with HWR. It is because when an AHBC with HWR corresponds to Fig. 3(e), the primary and secondary of the transformer are decoupled, and a voltage of $-V_o$ is applied to the output inductor.

Meanwhile, according to [8], considering the current ripple of the output inductor, Δi_{Lo}, the ZVS condition of an AHBC with FWR can be written as

$$L_{lk}>\frac{2C_{oss}}{\left(\frac{DT_s}{2L_m}+\frac{2I_o D}{n(1-D)V_g}-\frac{\Delta i_{Lo}}{n(1-D)V_g}\right)^2}\,. \tag{14}$$

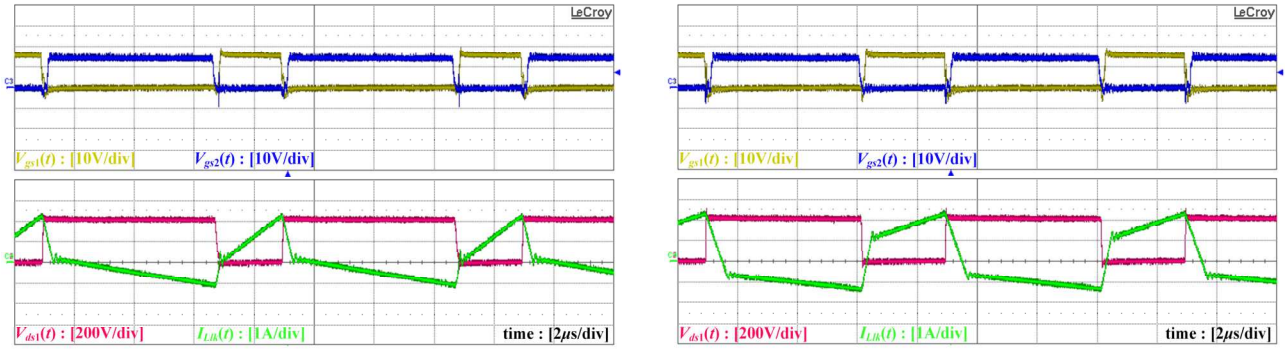

(a) (b)

Fig. 7. Experimental waveform of an AHBC with HWR. (a) 30% load condition, (b) 100% load condition.

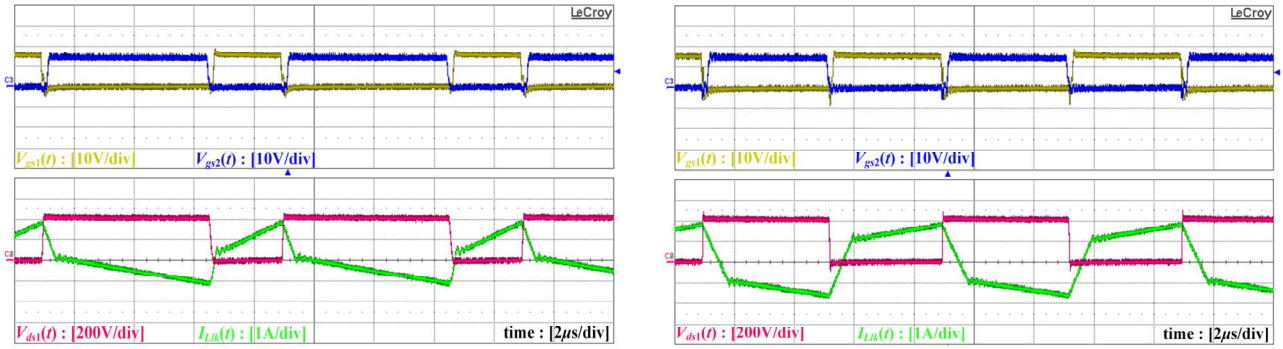

(a) (b)

Fig. 8. Experimental waveform of an AHBC with FWR. (a) 30% load condition, (b) 100% load condition.

In order to compare the soft switching characteristic of the two converters, they are designed under specific conditions in Table I, and the design results are shown in Table II. The minimum L_{lk} that can be used to achieve ZVS is calculated differently for each load current according to (12) and (14). Here, the results for 30% load condition and 100% condition are shown in Fig. 6(a) and Fig. 6(b), respectively. As shown in Fig. 6(a) and Fig. 6(b), an AHBC with HWR can attain ZVS by using a smaller L_{lk} under the same L_m condition, which is advantageous in soft switching. Additionally, designing with a smaller L_{lk} can improve efficiency in high-current applications by reducing duty cycle loss.

IV. Experimental Results

A 360-W (24 V/15 A) prototype was manufactured, and an experiment was conducted to verify the analysis. The design was made under the conditions of Table I, and the prototypes were built according to the results of Table II. Regarding the selection of semiconductor devices, SIHG14N50D was used for the bridge switches, and STPS30SM120ST was used for the output diodes D_1 and D_2. For an AHBC with HWR, L_m and L_{lk} were designed as 450 μH and 18 μH, respectively, to achieve ZVS under load conditions of 30% or higher. For an AHBC with FWR, they were designed as 450 μH and 27 μH, respectively, to achieve the same soft switching characteristics.

Fig. 7(a) and Fig. 7(b) show the experimental waveforms of an AHBC with HWR at 30% load and 100% load conditions, respectively. Even with smaller leakage inductance, an AHBC with HWR achieves soft switching under load conditions above 30%.

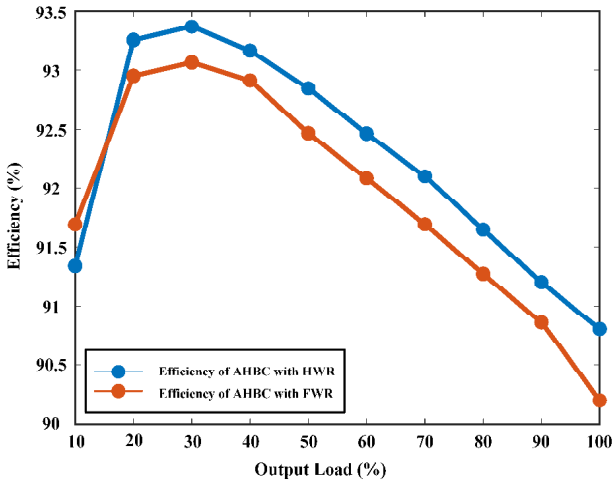

Fig. 9. Measured efficiency.

Meanwhile, Fig. 8(a) and Fig. 8(b) show the experimental waveforms of an AHBC with FWR at 30% load and 100% load conditions, respectively. It also performs ZVS as L_m and L_{lk} are designed to achieve soft switching under load conditions above 30%. However, it can be seen from the experimental waveform that the duty cycle loss significantly increased as the load increased since a relatively large L_{lk} was used to achieve ZVS. This can ultimately lead to reduced efficiency at heavy load conditions and means that the use of FWRs in high-current applications may be limited. Therefore, under the same L_m and V_{Cb} conditions, using HWR is desirable regarding converter design and efficiency.

Fig. 9 shows the measured converter efficiency for each load. According to the experimental results, the case

of using HWR showed better efficiency from light load to heavy load than the case of using FWR.

V. CONCLUSIONS

This study examines the superiority of an AHBC with an HWR in an efficiency aspect compared to the case of using an FWR through the operation characteristic analysis. Because the transformer current has a negative average with the reduced duty cycle loss due to the operation characteristics of an HWR, an AHBC with HWR can improve soft switching characteristics while maintaining appropriate conduction loss. Experiment results with a 360-W (24-V/15-A) prototype verified that the AHBC with an HWR could achieve ZVS of the main switch more efficiently and achieve high efficiency compared to the case of using an FWR throughout the whole load range.

ACKNOWLEDGMENT

This work was supported by project for the Industry-University-Research Institute platform cooperation R&D funded Korea Ministry of SMEs and Startups in 2022. (S3311623)

REFERENCES

[1] Jian Sun and V. Mehrotra, "Unified analysis of half-bridge converters with current-doubler rectifier," *APEC 2001. Sixteenth Annual IEEE Applied Power Electronics Conference and Exposition (Cat. No.01CH37181)*, 2001, pp. 514-520.

[2] Yu-Chieh Hung, Fu-San Shyu, Chih Jung Lin, and Yen-Shin Lai, "Design and implementation of symmetrical half-bridge DC-DC converter," *The Fifth International Conference on Power Electronics and Drive Systems, 2003. PEDS 2003.*, 2003, pp. 338-342.

[3] Weiyun Chen, Peng Xu and F. C. Lee, "The optimization of asymmetric half bridge converter," *APEC 2001. Sixteenth Annual IEEE Applied Power Electronics Conference and Exposition (Cat. No.01CH37181)*, Anaheim, CA, USA, 2001, pp. 703-707.

[4] V. Meleshin and D. Ovchinnikov, "Improved Asymmetrical Half-Bridge Converters," *2005 International Conference on Power Electronics and Drives Systems*, Kuala Lumpur, Malaysia, 2005, pp. 401-406.

[5] W. Eberle, Yongtao Han, Yan-Fei Liu and Sheng Ye, "An overall study of the asymmetrical half-bridge with unbalanced transformer turns under current mode control," *Nineteenth Annual IEEE Applied Power Electronics Conference and Exposition, 2004. APEC '04.*, Anaheim, CA, USA, 2004, pp. 1083-1089.

[6] R. Miftakhutdinov, A. Nemchinov, V. Meleshin and S. Fraidlin, "Modified asymmetrical ZVS half-bridge DC-DC converter," APEC '99. Fourteenth Annual Applied Power Electronics Conference and Exposition. 1999 Conference Proceedings (Cat. No.99CH36285), Dallas, TX, USA, 1999, pp. 567-574.

[7] Hong Mao, Songquan Deng, J. Abu-Qahouq and I. Batarseh, "Active-clamp snubbers for isolated half-bridge DC-DC converters," in *IEEE Transactions on Power Electronics*, vol. 20, no. 6, pp. 1294-1302, Nov. 2005.

[8] H. Choi, "Design considerations for asymmetric half-bridge converter", *Fairchild Semiconductor Power Seminar*, Phoenix, AZ, USA, 2009, pp.1-16.